ISBN: 978-3-95450-232-5 ISSN: 2673-7000 doi:10.18429/JACoW-NAPAC2022-TUPA64

ANALYSIS OF RESONANT CONVERTER TOPOLOGY FOR HIGH-VOLTAGE MODULATORS*

M. S. Barrueta†, M. Morris, J. Lyles
Los Alamos National Laboratory, Los Alamos, NM 87545, USA

Abstract

At the Los Alamos Neutron Science Center (LANSCE), we are considering various topologies to replace obsolete charging supplies and capacitor banks that provide high-voltage direct-current (DC) power to the 44, 805-MHz klystron modulators that drive the LANSCE Coupled Cavity Linac (CCL). Among the possible replacement topologies is the High Voltage Converter Modulator (HVCM), originally designed at LANSCE for use at the Spallation Neutron Source (SNS), to be used as a pulsed high-voltage power supply for klystron-based RF transmitters. The HVCM topology uses high frequency transformers with resonant LC networks for efficient energy conversion and a frequency dependent gain, which permits the use of frequency modulation as a control variable to afford pulse flattening and excellent regulation as demonstrated at SNS. A mathematical analysis is presented that links the converter resonant tank components to the frequency dependent output behaviour of the converter modulator.

INTRODUCTION AND PURPOSE

The LANSCE CCL is currently celebrating its 50-year anniversary since it first accelerated beam. Since its design, the system has largely remained unchanged with the exception of some life extension programs [1, 2]. In this aging system, component obsolescence is becoming an increasing problem, especially in the high voltage power supply. We are currently considering long pulse power converters such as the SNS High Voltage Converter Modulator (HVCM) [3, 4] or the ESS stacked multilevel (SML) modulator [5].

High power klystrons that can produce multiple MW of output peak power, typically require levels of around 100 kV of cathode voltage and several tens of Amperes of peak current to operate. Due to the current availability of solid-state switches, a pulsed voltage/current of this magnitude cannot be obtained in a single "boost" converter without parallel/series combination of the switches, therefore, designers use different techniques to produce the necessary output pulses. The SML modulator developed by ESS relies on series combination of output stages that combine to deliver the necessary voltage. The HVCM modulator currently used at SNS uses a quasi-resonant circuit to enhance the voltage gain already offered by the output transformer.

Multiple publications exist describing the behaviour of resonant converters, but none of these describes the operation of the HVCM converter modulator, which has high oscillating currents in the transformer's primary and cannot reliably add a series resonating capacitor due to its high peak power operation. This paper presents a mathematical analysis of an HVCM style pulsed power source.

TOPOLOGY AND ANALYSIS

The HVCM is composed of a full bridge Insulated Gate Bipolar Transistor (IGBT) input feeding a "boost" transformer (represented by its series and magnetizing inductance model) that in turn feeds a capacitor in parallel with a full bridge rectifier. The rectified output is connected to the load, in this case, one or several klystrons connected in parallel. This circuit is shown in Figure 1.

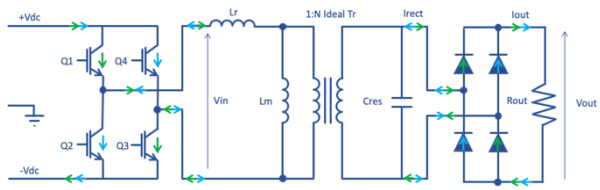

Figure 1: HVCM topology. Current directions in alternate cycles are shown in green or blue.

The First Harmonic Approximation (FHA), a method typically used in the analysis of resonant converters [6, 7] assumes that input to output power transfer is mainly due to the fundamental of the Fourier series components of voltages and currents. It provides a simplified method to examine resonant converters in the frequencies around resonance which is typically where these topologies are operated.

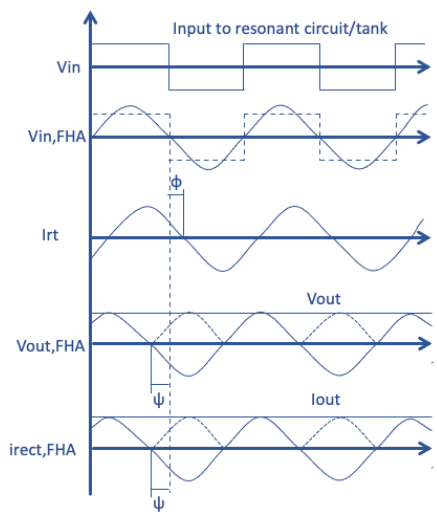

Figure 2: HVCM input and output waveforms and FHA simplification.

* Work supported by the United States Department of Energy, National Nuclear Agency, under contract No. 89233218CNA000001.
† maria.sanchez.barrueta@lanl.gov

ISBN: 978-3-95450-232-5 ISSN: 2673-7000 doi:10.18429/JACoW-NAPAC2022-TUPAC64

It can be easily seen that through the FHA analysis, the input and output waveforms of the HVCM will be as shown in Figure 2. The following are the Fourier series corresponding to each of the waveforms:

$$v_{in}(t) = \frac{4}{\pi}\sum_{n=1,3,5\ldots}\frac{1}{n}V_{dc}\sin(2\pi\cdot f_{sw}\cdot t) \quad (1)$$

$$i_{in}(t) = \sqrt{2}\sum_{n=1,3,5\ldots}\frac{1}{n}I_{rt}\,sin(2\pi\cdot f_{sw}\cdot t+\varphi) \quad (2)$$

$$v_{out}(t) = \frac{4}{\pi}\sum_{n=1,3,5\ldots}\frac{1}{n}V_{out}\sin(2\pi\cdot f_{sw}\cdot t-\psi) \quad (3)$$

$$i_{rect}(t) = \sqrt{2}\sum_{n=1,3,5\ldots}\frac{1}{n}I_{rect}\,sin(2\pi\cdot f_{sw}\cdot t-\psi) \quad (4)$$

Extracting the first harmonic out of the Fourier series and performing some simple transformations we obtain the rms values of the input waveforms:

$$V_{in,FHA} = \frac{2\sqrt{2}}{\pi}V_{dc} \quad (5)$$

$$I_{dc} = \frac{2\sqrt{2}}{\pi}\,I_{rt}\cos\varphi \quad (6)$$

Based on the output filtering [8], the output waveforms rms values can also be obtained:

$$V_{out,FHA} = \frac{2\sqrt{2}}{\pi}V_{out} \quad (7)$$

$$I_{rect,FHA} = \frac{2\sqrt{2}}{\pi}\,I_{rect} \quad (8)$$

$$I_{out} = \frac{2}{T_{sw}}\int_0^{\frac{T_{sw}}{2}}\left|i_{rect,FHA}(t)\right|dt = \frac{2\sqrt{2}}{\pi}\,I_{rect} = \frac{V_{out}}{R_{out}} \quad (9)$$

An alternate current equivalent of the output rectifier and load can be calculated:

$$R_{o,ac} = \frac{V_{out,FHA}}{I_{rect}} = \frac{\frac{2\sqrt{2}}{\pi}V_{out}}{\frac{\pi\sqrt{2}V_{out}}{4\ R_{out}}} = \frac{8}{\pi^2}R_{out} \quad (10)$$

FHA therefore allows for the initial circuit displayed in Figure 1 to be simplified down to a circuit entirely composed by ac sources and complex impedances, as the one in Figure 3.

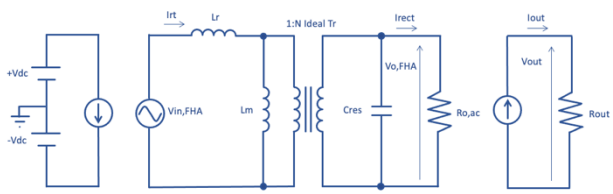

Figure 3: First harmonic analysis simplification.

Further simplification can be obtained by moving the capacitance and load to the primary of the transformer:

$$C_{eq} = N^2C_{res} \quad (11)$$

$$R_{eq} = \frac{R_{o,ac}}{N^2} \quad (12)$$

The resulting simplified model, shown in Figure 4, provides insight into the frequency dependent behavior of the HVCM.

Gain

The relationship between V_{in} and V_{out} can be established from the circuit in Figure 4 through a simple voltage

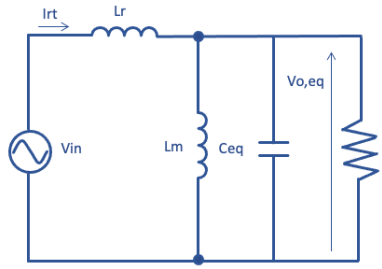

Figure 4: AC model of HVCM.

divider circuit:

$$Gain = \frac{V_{out}}{V_{dc}} = \frac{\frac{\pi}{2\sqrt{2}}V_{out,FHA}}{\frac{\pi}{2\sqrt{2}}V_{in,FHA}} = \frac{V_{out,FHA}}{V_{in,FHA}} = N\frac{V_{o,eq}}{V_{in,FHA}} \quad (13)$$

$$G(\omega) = \frac{V_{o,eq}}{V_{in,FHA}} = \frac{R_{eq}//C_{eq}//L_m}{j\omega L_r+R_{eq}//C_{eq}//L_m} \quad (14)$$

A useful parametrization is to relate the circuit's behavior to the resonant frequency due to the L_r and C_{eq} interaction:

$$\lambda = \frac{L_r}{L_m} \quad (15)$$

$$f_r = \frac{1}{2\pi\sqrt{C_{eq}L_r}} \quad (16)$$

$$f_n = \frac{f}{f_r} \quad (17)$$

$$Z_o = \sqrt{\frac{L_r}{C_{eq}}} = 2\pi\cdot f_r\cdot L_r = \frac{1}{2\pi\cdot f_r\cdot C_{eq}} \quad (18)$$

$$Q = \frac{Z_o}{R_{eq}} \quad (19)$$

Applying these conversions, we obtain:

$$G(f_n) = \frac{1}{jQf_n+\lambda-{f_n}^2+1} \quad (20)$$

Input impedance

Other than the given Zero Current Switching (ZCS) naturally performed by the rectification stage of a converter, resonant converters allow for Zero Voltage Switching (ZVS) to occur, reducing the switch on losses of the solid-state switches [4, 5]. ZVS is possible through a resonant phenomenon of the circuit and the parasitic capacitance of the solid-state switches. For this to occur, the input current must lead the input voltage, or in other terms, the input impedance of the circuit must be inductive.

$$Z_{in}(\omega) = \frac{V_{in}}{I_{rt}} = j\omega L_r + R_{eq}//C_{eq}//L_m \quad (21)$$

$$Z_{in}(f_n) = Z_o f_n\frac{-Qf_n+j(\lambda-{f_n}^2+1)}{(\lambda-{f_n}^2)+jQf_n} \quad (22)$$

$$\varphi = \tan^{-1}\left(\frac{-\lambda+{f_n}^2-1}{Qf_n}\right)-\tan^{-1}\left(\frac{Qf_n}{Q\lambda-{f_n}^2}\right) \quad (23)$$

Frequency, load and inductance dependence

As shown in the previous equations, both the input impedance and the voltage gain vary with frequency, loading and the ratio of inductance. Figure 5 shows how the changing inductance ratio λ affects voltage gain behavior with

ISBN: 978-3-95450-232-5 ISSN: 2673-7000 doi:10.18429/JACoW-NAPAC2022-TUPA64

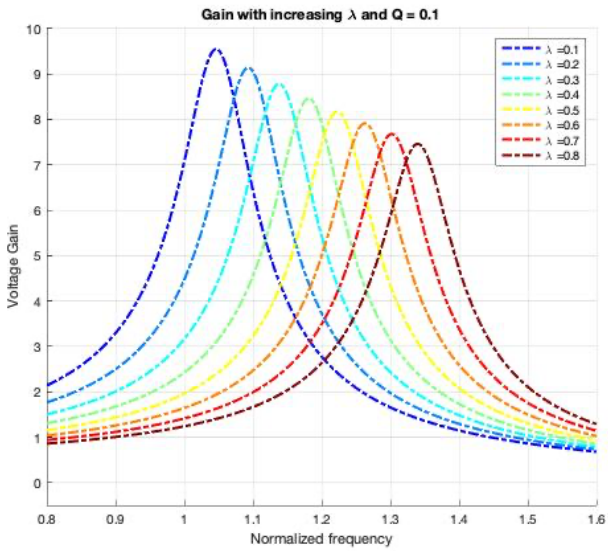

Figure 5: Voltage gain across HVCM for different values of λ.

frequency. Essentially, the more significant the magnetizing inductance, the higher the resonant frequency and lower maximum voltage gain at resonance.

A similar analysis applied to the variation with loading (Q=0, open circuit) reveals that the higher the Q, the lower the voltage gain at resonance. This can be seen in Figure 6 as well as the limits of inductive and capacitive regions for every curve, limiting the frequency for ZVS operation.

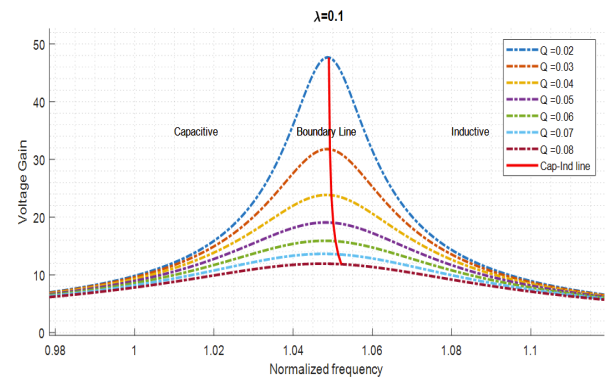

Figure 6: Voltage gain across HVCM for different levels of loading superimposed with inductive/capacitive regions.

Comparison with LLC converter

A traditional resonant converter uses a series resonant capacitor rather than one parallel with the output (circuit presented in Figure 8). This topology has a frequency response presenting a double resonance. One resonant frequency corresponds to the series resonance (L_r and C_r resonate) while the other matches parallel resonance (L_r+ L_m with C_r). One of the greatest advantages of this topology is that at series resonance, the LLC converter has a load independent behavior (see Figure 7). Since the impedance of the series circuit is zero at resonance, the voltage gain at this point is only unity. In an application such as the HVCM, where a considerable voltage gain is necessary, operation around series resonance would not be useful.

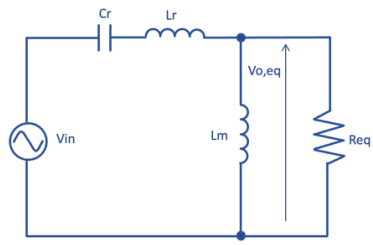

Figure 8: Typical LLC resonant converter.

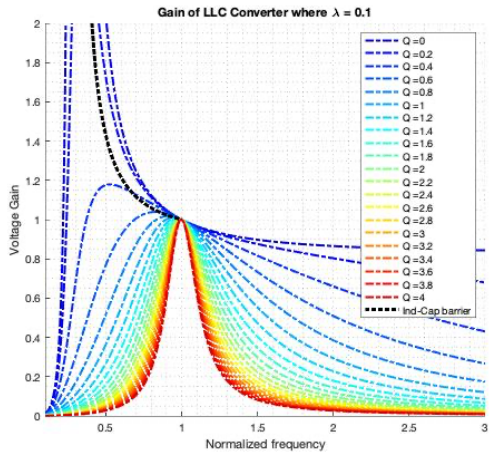

Figure 9: Voltage gain response of a traditional LLC converter.

One could anticipate that since the LLC converter and the HVCM have the same number of components, their operation would be alike, but it seems that the HVCM operates similarly to the series resonant converter which corresponds to the specific case of λ=0 in Eq. (20). This relationship is shown in Figure 10.

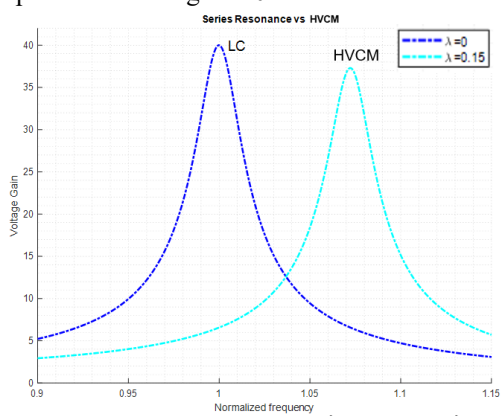

Figure 10: HVCM converter vs. series resonant converter.

CONCLUSION

A mathematical analysis of the voltage gain and the input impedance of the HVCM style converter is presented, based on a FHA approach. A comparison with a popular choice of topology in resonant converters and a similar operation converter reveals that the HVCM does not operate like an LLC converter, but rather as a frequency shifted series converter.

ISBN: 978-3-95450-232-5 ISSN: 2673-7000 doi:10.18429/JACoW-NAPAC2022-TUPA64

REFERENCES

[1] D. E. Rees *et al.*, "LANSCE RF System Refurbishment", in *Proc. PAC'07*, Knoxville, TN, USA, May 2007, pp. 2476-2478. doi:10.1109/PAC.2007.4441263

[2] W. A. Reass, D. M. Baca, J. L. Davies, and D. E. Rees, "Pulsed Klystrons with Feedback Controlled Mod-anode Modulators", in *2009 IET European Pulsed Power Conference*, Geneva, Switzerland, Sep. 2009, pp. 1-4. doi:10.1049/CP.2009.1675

[3] W. A. Reass. *et al*., "Design, Status, and First Operation of the Spallation Neutron Source Polyphase Resonant Converter Modulator System", in *Proc. PAC'03*, Portland, OR, USA, May 2003, pp. 553-557. doi:10.1109/PAC.2003.1288975

[4] D. J. Solley and D. E. Anderson, "Updates on the Progress of the Alternate Topology Modulator (AT-HVCM) to support the Proton Power Upgrade (PPU) at the Spallation Neutron Source", in *Proc. IPMHVC'18*, Jackson, WY, USA, Jun. 2018, pp. 75-80. doi:10.1109/IPMHVC.2018.8936700

[5] C. A. Martins and M. Collins, "Optimal Design of a High-Voltage DC/DC Converter for the 11.5-MW/115-kV ESS Long-Pulse Modulator", *IEEE Trans. Plasma Sci.*, vol. 48, pp. 3332-3341, 2020. doi:10.1109/TPS.2020.2991451

[6] S. De Simone, C. Adragna, C. Spini, and G. Gattavari, "Design-oriented steady-state analysis of LLC resonant converters based on FHA", in *Proc. SPEEDAM'06*, Taormina, Italy, 2006, pp. 200-207. doi:10.1109/SPEEDAM.2006.1649771

[7] Y. Shen, W. Zhao, Z. Chen, and C. Cai, "Full-Bridge LLC Resonant Converter with Series-Parallel Connected Transformers for Electric Vehicle On-Board Charger", *IEEE Access*, vol. 6, pp. 13490-13500, 2018. doi:10.1109/ACCESS.2018.2811760

[8] R. L. Steigerwald, "A comparison of half-bridge resonant converter topologies", *IEEE Trans. Power Electron.*, vol. 3, pp. 174-182, 1988. doi:10.1109/63.4347